ELSEVIER

Journal of Hazardous Materials B138 (2006) 160–168

Journal of Hazardous Materials

www.elsevier.com/locate/jhazmat

Optimization of integrated chemical–biological degradation of a reactive azo dye using response surface methodology

Gatut Sudarjanto, Beatrice Keller-Lehmann, Jurg Keller*

Advanced Wastewater Management Centre, The University of Queensland, Qld 4072, Australia

Received 13 December 2005; received in revised form 17 May 2006; accepted 17 May 2006
Available online 26 May 2006

Abstract

The integrated chemical–biological degradation combining advanced oxidation by UV/H_2O_2 followed by aerobic biodegradation was used to degrade C.I. Reactive Azo Red 195A, commonly used in the textile industry in Australia. An experimental design based on the response surface method was applied to evaluate the interactive effects of influencing factors (UV irradiation time, initial hydrogen peroxide dosage and recirculation ratio of the system) on decolourisation efficiency and optimizing the operating conditions of the treatment process. The effects were determined by the measurement of dye concentration and soluble chemical oxygen demand (S-COD). The results showed that the dye and S-COD removal were affected by all factors individually and interactively. Maximal colour degradation performance was predicted, and experimentally validated, with no recirculation, 30 min UV irradiation and 500 mg H_2O_2/L. The model predictions for colour removal, based on a three-factor/five-level Box–Wilson central composite design and the response surface method analysis, were found to be very close to additional experimental results obtained under near optimal conditions. This demonstrates the benefits of this approach in achieving good predictions while minimising the number of experiments required.

Keywords: Textile dye; Colour removal; UV/H_2O_2; Chemical–biological process; Response surface methodology

1. Introduction

Synthetic dyes are produced and consumed annually in large quantities in different kinds of industries, such as textile, food processing, leather/tanning, pulp and paper, cosmetics and pharmaceutical industries. The textile industry accounts for two-thirds of the total dyestuff market [1], consuming a large quantity of reactive dyes with azo-based chromophores due to the high demand for cotton fabrics with brilliant colours [2]. Therefore, large amounts of coloured wastewater that contain synthetic dyes are generated by the textile industry. In many cases this kind of wastewater is aesthetically unacceptable, hinders light penetration, damages the quality of the receiving streams, and may be inhibitory towards biological wastewater treatment systems (due to its complex chemical structure), to food chain organisms and to aquatic life. Consequently, it is important to remove dyestuff from the wastewater before discharging it to the environment. Conventional activated sludge systems have difficulty in handling such wastewater, particularly in removing the colour. Ineffective treatment by conventional systems can cause the release of 20–50% of unfixed dyes into the environment [3]. Coagulation/flocculation and other conventional physical–chemical techniques are known to be costly and only transfer the pollutants from the liquid to the solid phase and thus other secondary problems arise. Therefore, a better and more appropriate method of handling coloured wastewater is needed.

Numerous advanced treatment technologies have been developed to reduce contaminants from textile wastewater. To effectively treat such wastewater, often a combined chemical and biological oxidation process is required as purely biological treatment is usually very slow or not possible at all. Advanced oxidation processes (AOPs) can improve the biodegradability of refractory organic compounds through the use of short-lived, very reactive hydroxyl radicals ($OH^{\bullet}$) [4–6]. Some examples of AOPs are the use of ozone (O_3) at elevated pH, UV/H_2O_2, UV/O_3, UV/TiO_2 and Fenton reagents (H_2O_2/Fe^{2+}). The UV/H_2O_2 method of treating textile wastewaters has the potential to degrade toxic and/or carcinogenic compounds effec-

* Corresponding author. Tel.: +61 7 33654727; fax: +61 7 33654726.
E-mail address: j.keller@awmc.uq.edu.au (J. Keller).

0304-3894/$ – see front matter © 2006 Elsevier B.V. All rights reserved.
doi:10.1016/j.jhazmat.2006.05.054

Nomenclature

ANOVA	analysis of variance
AOP	advanced oxidation process
CCD	central composite design
d.f.	degrees of freedom
F-value	Fischer's value
MBBR	moving bed biofilm reactor
Pr	probability
R^2	square of the correlation coefficient
RR195A	Reactive Red 195A
RSM	response surface methodology
RSREG	response surface regression
SAS	statistical analysis software
S-COD	soluble chemical oxygen demand (mg/L)
X_1	UV irradiation (min)
X_2	initial H_2O_2 dosage (mg/L)
X_3	recirculation ratio (%)
Y_1	predicted dye response (%)
Y_2	predicted S-COD response (%)

Greek letters

β_0	constant coefficient (intercept)
β_i	linear coefficients
β_{ii}	quadratic coefficients
β_{ij}	crossproduct coefficients
λ	wavelength (nm)

tively. In this process, stable organic compounds with high molecular weights are broken down into smaller structures, which are more biodegradable [7]. The treated effluent does not contain sludge [8] and foul odours are greatly reduced [9]. In addition, compared to the other AOPs, the UV/H_2O_2 method offers several practical advantages as H_2O_2 is commercially available, easy to handle and fully dissolves in water without any phase transfer problems. Furthermore, the method also has simplicity of operation and lower investment costs [10,11] compared with energy-intense AOPs such as power ultrasound or combinations of ozone and UV irradiation. Nevertheless, total mineralization is quite difficult to achieve except when long reaction times are applied in the system.

Aerobic biological processes are efficient and cost-effective for smaller molecules which are usually produced from the AOP operation. The aerobic biofilm reactor (also called moving bed biofilm reactor, MBBR) is an effective technique to treat industrial wastewater. The system is known to achieve high volumetric loads, no washout problems and a compact design of the reactor [12]. The combined AOP/bioreactor process is expected to be more economic and effective compared to any single treatment technology to achieve the same level of treatment.

In the present study, the ability of the integrated UV/H_2O_2 and aerobic biological process were examined to decolourise a reactive azo dye. There are some factors that may significantly influence the degradation process, such as pH, temperature, initial H_2O_2 dosage, UV irradiation time, recirculation ratio from the bioreactor to the UV photoreactor, hydraulic retention time in the bioreactor, etc. Process optimization could be done by empirical or statistical methods. The empirical method is time consuming and does not necessarily enable an effective optimization. A statistical-based technique commonly called the response surface method (RSM) as a powerful experimental design tool has been used to optimize and understand the performance of complex systems [13–15]. The RSM was developed by [16] and represents a compilation of experimental design and multiple regression-based methods that can be applied to examine problems where several factors might affect a response [17]. In this study, the Box–Wilson statistical design method was used as a design framework for second-order response surface modeling to evaluate dependent variables as functions of independent variables or factors.

2. Materials and methods

2.1. Reagents

The dye chosen for the study was C.I. (Colour Index) Reactive Azo Red 195A or RR195A (Recochem, Australia). The known structure of the vinylsulphone mono azo dye is presented in Fig. 1. The dye was obtained from the Logan Textile Company, Qld, Australia, as a commercial product that is regularly utilized by the company without further purification (dye purity was around 70%). The molecular weight of the dye was 1025 g/mol with maximum absorption at $\lambda = 542$ nm. In the real dyeing process, the dye is hydrolysed prior to its application to promote the reaction between dye and fiber. In the present study, the hydrolysed dye stock solution was prepared according to the common dyebath application conditions recommended by the textile company. Five grams of dye and 40 g of NaOH were dissolved in approximately 500 mL of MilliQ® water and the pH was adjusted to 12 with 1 M NaOH solution. The solution was stirred for 1 h at 80 °C. After cooling to room temperature, the solution was neutralized to pH 7 with H_2SO_4 and diluted to 1 L with MilliQ® water. The dye was used as the sole carbon source with a concentration of 90–100 mg/L as soluble chemical oxygen demand (S-COD). Small quantities of nutrients (KH_2PO_4 and $(NH_4)_2SO_4$) required by the microorganism in the bioreactor were added to the wastewater in the feed tank at a COD:N:P ratio of 200:5:1. This was done as a precaution to avoid any possible nutrient limitations in these experiments but is not considered necessary in a process application. Trace elements such as Cu, Mn, Zn, Mg, and Ca were also included but no specific

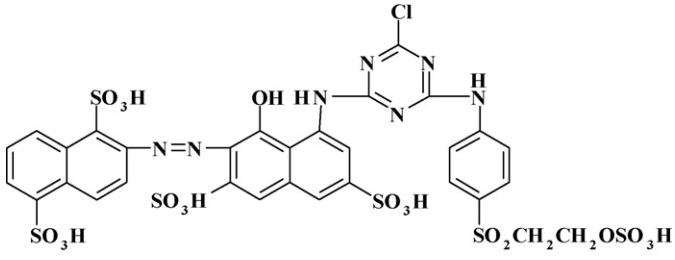

Fig. 1. Chemical structure of C.I. Reactive Red 195A.

pH buffer was added. Analytical grade H_2O_2 (30%, w/w) was obtained from Merck (Germany) and used without further purification. The pH was adjusted to the desired value using H_2SO_4 and NaOH. All other chemicals were of reagent grade quality and solutions were prepared with MilliQ® water.

2.2. Reactor configuration

The reactions were carried out in two different reactors, the photoreactor and the bioreactor, which were operated in series (Fig. 2). The photoreactor was an Ultraviolet Technology of Australasia (UVTA) model LC-20 with the total volume of 585 mL, which is one of a family of UV disinfection units manufactured by UVTA Pty. Ltd. (Australia). The UV light irradiates the simulated wastewater as it flows through the activated fluoropolymer (AFP840) tubing within the unit. The AFP840 teflon type tube is transparent, non-wettable, and chemically inert. The photoreactor is fitted with a fixed low-pressure mercury lamp (60 W emitting at 253.7 nm) with a UV intensity rating of more than 34 mW/cm^2 (manufacturer's specification). The UV lamp and the AFP tube are covered by a metal casing. The lamp was warmed up for a few minutes before H_2O_2 was added to get a constant UV flux and eliminate temperature variations.

The 5-L cylindrical bioreactor was placed after the photoreactor and aerated continuously. Plastic carriers (Kaldnes K1 and Anox Biochips, AnoxKaldnes AB, Lund, Sweden) were suspended in the bioreactor to foster the growth of microbial biofilms. As this is a biofilm process, information on the "sludge age" or biomass concentration cannot be readily obtained. However, only small amounts of biomass were generated in the process due to the low loading and limited biodegradability, forming a thin biofilm on the carrier material. Partially degraded dye wastewater from the UV/H_2O_2 treatment process that still contained residual hydrogen peroxide was added into the bioreactor to acclimatize the microorganisms to this particular wastewater. The reactor influent was supplemented with increasing concentrations of residual H_2O_2, beginning at a level of 50 mg H_2O_2/L influent to 200 mg H_2O_2/L influent. The acclimatization process at a hydraulic retention time of 10 h was completed after a period of 3 months when steady state conditions were achieved. The concentration of dissolved oxygen (DO) was monitored continuously and controlled automatically to ensure aerobic conditions in the bioreactor. The general schematic diagram of the integrated treatment process is depicted in Fig. 2. All experiments were performed under continuous operation of the whole process. Steady state conditions in the system were considered to be achieved after three hydraulic retention times of the bioreactor (30 h) after which triplicate samples (over a 2 h period) were collected at each experimental condition.

In this study, some important parameters (initial H_2O_2 dosage, UV irradiation time and recirculation from the bioreactor to the photoreactor) were varied to determine the optimum condition of the treatment process in degrading RR195A. Meanwhile, the initial pH of the influent (pH 8), temperature (30 °C), dye concentration (100 mg/L) and hydraulic retention time of the bioreactor (10 h) were kept constant to reduce the number of factors and to simplify the experimental design. The selection of factors and the chosen levels were determined based on previous studies [18,19] and initial screening experiments of various parameters and different levels.

The initial H_2O_2 concentration was varied from 100 to 500 mg H_2O_2/L of dye solution fed to the photoreactor, UV irradiation of 10–30 min and a recirculation ratio between 0% (no recirculation) and 600% (or six times relative to the influent flow

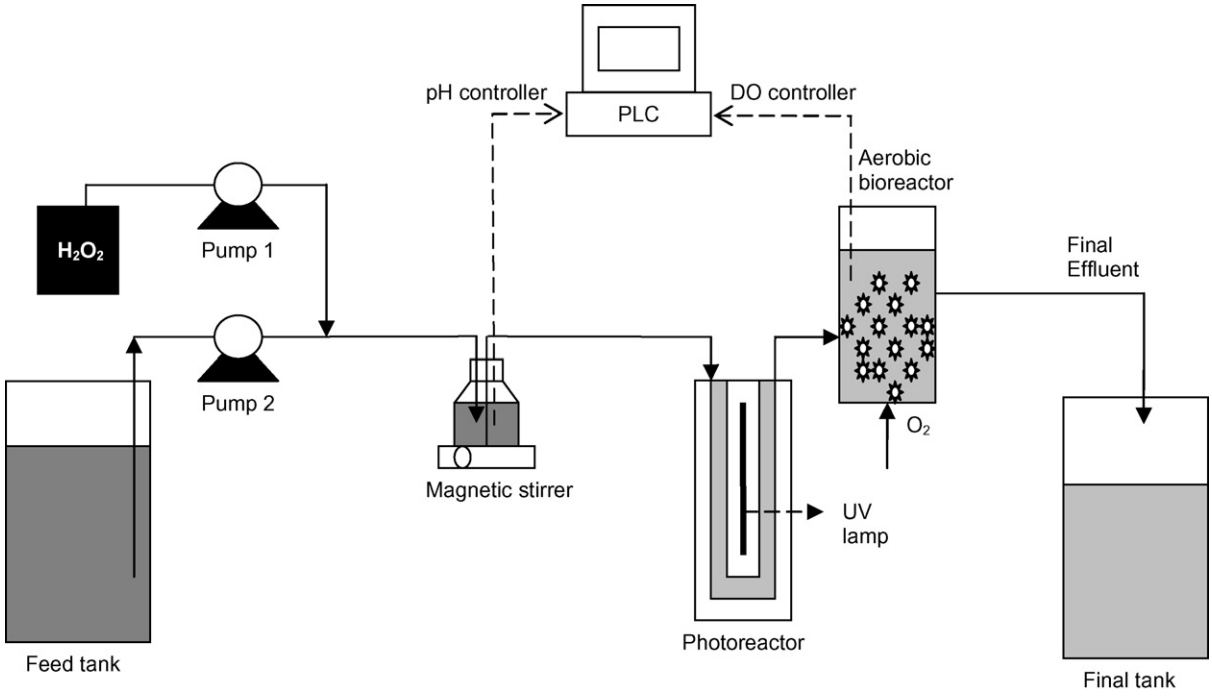

Fig. 2. Schematic diagram of the integrated treatment process.

rate). The maximal H_2O_2 concentration and UV irradiation time were determined from the near complete dye degradation (based on spectrophotometric measurements) that could be achieved at these levels in the screening experiments ([18], data not shown).

2.3. Analytical methods

H_2O_2 concentration was determined by Reflectoquant Peroxide test strips (Merck, Germany). Residual H_2O_2 was eliminated before the soluble chemical oxygen demand (S-COD) measurement to avoid incorrect results. 100 μL catalase solution, which was prepared by adding 500 μL of catalase from bovine liver (C100, Sigma–Aldrich) in 100 mL of 0.05 M potassium phosphate buffer, pH 7 [20], was added to each sample after the neutralization with NaOH or HCl. A spectrophotometric method [21] using Photometer SQ 118 (Merck, Germany) with a wavelength of 550nm was used to measure the dye concentration from filtered samples. S-COD was measured according to Standard Methods [21] using commercially available chemicals (COD range 10–150 mg/L) and Thermoreactor TR 300 (both Merck, Germany), with absorbance measurements made using the Photometer SQ 118 (Merck, Germany). The pH level of the influent to the reactors was adjusted to eight and automatically controlled through acid or base addition. Samples were taken at predetermined reaction times to measure dye and S-COD concentrations. All samples were filtered using a syringe filter (0.22 μm Millex® GP, Bedford, USA) and diluted where necessary before analysis. Simulated wastewater was prepared immediately before irradiation.

2.4. Experimental design

Optimization of the integrated chemical–biological treatment process to degrade RR195A was carried out using the RSM design [17]. The objective of the RSM is to estimate interaction and the quadratic effects as well as giving an idea of the local shape of the response surface we were examining. A further benefit of using the RSM design is the reduction of the number of experiments needed compared to a full experimental design at the same level.

A three-factor and a five-level Box–Wilson central composite design (CCD) consisting of fourteen experimental runs was performed including six replicates at the centre point. The design contains three major components. The first is an embedded factorial with two levels of each of the factors coded as −1 and +1. The second component of the design is the star points. There must be sufficient of these to allow estimation of the curvature of the model and preferably be chosen so that the standard error of the response variable is the same at any point of the fitted surface. In this case, this was achieved by selecting six points equally spaced around the circumference of a circle with a radius alpha, where alpha is equal to ±1.682. As the factorial and star experimental combinations are not replicated, a number of centre points are added as the third component in order to provide degrees of freedom for estimating experimental error and also to determine the precision of the response variable near the centre. The number of centre points is chosen so that the standard error of the estimate of the response variable is approximately the same at the centre as at all points in the circle with radius 1. This arbitrary order is then randomized to produce the run order using Minitab statistical software (Minitab® R14). In the present study, the UV irradiation time (X_1, min), initial H_2O_2 dosage (X_2, mg/L), and recirculation ratio (X_3, %) were considered as independent factors and colour removal (Y_1, %) and S-COD removal (Y_2, %) were considered as dependent factors. The levels of independent factors were selected based on values obtained in preliminary experiments. These levels were chosen to be within the range of reasonable formulations, since interpretation of the results was valid only within the experimental limits. The UV irradiation (X_1) was varied between 10 and 30 min, the initial H_2O_2 dosage (X_2) between 100 and 500 mg/L and the recirculation ratio (X_3) between 0 and 600%.

2.5. Data analysis

Experimental data were analysed using the response surface regression (RSREG) procedure of the statistical analysis system (SAS version 8) and fitted to a second-order polynomial model. The following response function (Eq. (1)) was used in the response surface analysis to correlate the dependent and independent factors

$$Y = \beta_0 + \sum_{i=1}^{3}\beta_i X_i + \sum_{i=1}^{3}\beta_{ii} X_i^2 + \sum_{i}\sum_{j=i+1}\beta_{ij} X_i X_j \quad (1)$$

where Y is the predicted response; β_0 the constant coefficient (intercept); β_i the linear coefficients; β_{ii} the quadratic coefficients; β_{ij} is the crossproduct coefficients. X_i and X_j are independent factors. Two-dimensional contour plots and three-dimensional curves of the response surfaces were developed using DPlot (version 1.997) software while holding a variable constant in the second-order polynomial model. The validity of the model was determined by comparing the experimental and predicted values. Furthermore, the predicted operating conditions for maximal dye removal were experimentally verified in an additional study.

3. Results and discussion

In general, the colour and S-COD removal efficiencies obtained from the experiments are influenced by all factors investigated, i.e. initial H_2O_2 dosage, UV irradiation time and recirculation ratio of the system, as well as some others, and their effects are either individual or interactive.

3.1. Fitting the models

The three independent factors for RSM as coded and uncoded values are shown in Table 1. The overall three-factor and five-level Box–Wilson central composite experimental design used for RSM and details of the experimental data for the removal efficiencies are shown in Table 2. The observed colour removal efficiencies varied between 20 and 86% and the model predictions matched the experimental results well. In terms of S-COD,

Table 1
Independent factors and their coded levels used for optimization

Independent factor	Units	Symbol	Coded levels				
			−1.682	−1	0	+1	+1.682
UV irradiation time	min	X_1	10	14	20	26	30
Initial H_2O_2 dosage	mg/L	X_2	100	181	300	419	500
Recirculation ratio	%	X_3	0	122	300	478	600

Table 2
Three-factor and five-level Box–Wilson central composite designs for RSM and the predicted and experimentally achieved removal efficiencies

Std order[a]	Run order[b]	UV irradiation (min)	Initial H_2O_2 (mg/L)	Recirculation ratio (%)	Dye removal (%)	Predicted response Y_1 (%)	S-COD removal (%)	Predicted response Y_2 (%)
1	19	14	181	122	33	36	10	9
2	10	26	181	122	45	52	16	21
3	5	14	419	122	52	51	18	13
4	2	26	419	122	66	68	25	19
5	18	14	181	478	24	25	9	20
6	4	26	181	478	26	30	12	23
7	13	14	419	478	35	31	19	20
8	20	26	419	478	38	38	10	17
9	3	10	300	300	28	30	7	11
10	1	30	300	300	57	49	19	17
11	17	20	100	300	20	19	3	7
12	7	20	500	300	16	38	12	6
13	11	20	300	0	86	72	39	29
14	12	20	300	600	25	38	13	36
15	14	20	300	300	44	37	16	14
16	16	20	300	300	40	37	14	14
17	9	20	300	300	36	37	14	14
18	8	20	300	300	35	37	14	14
19	6	20	300	300	35	37	11	14
20	15	20	300	300	35	37	11	14

[a] Non-randomized.
[b] Randomized.

the removal efficiencies varied between 3 and 39%. However, a number of experimental results were not predicted well by the model (particularly experiments 5, 6 and 14, Table 7), possibly due to the limited range of removal efficiencies under the experimental conditions. These results clearly indicate that the chosen factors had a major influence on the treatment performance. Experimental data were used in RSREG procedure of SAS to find the coefficients of the response function. The coefficients of the response function for colour and S-COD removal efficiencies are listed in Table 3. The significance of all experimental factors that affect the treatment process performance can be justified from the model coefficients, multiple determinations and probabilities that were generated from the RSREG procedure of SAS software. In optimizing a response surface, an adequate fit of the model should be obtained to avoid poor or ambiguous results [22]. This is important to ensure the adequacy of the proposed model. Table 4 demonstrates that the lack of fit of both colour and S-COD removal efficiency models were significant. Furthermore, as the crossproduct of both models did not fit the data very well, firm statements about the processes should not be based only on the current analysis.

Table 5 shows the analysis of variance of the regression parameters of the predicted response surface quadratic models for colour and S-COD removal efficiencies by the integrated treatment process. As can be seen, both linear and quadratic parameters were very significant with Pr (probability) < 0.001 (linear), Pr < 0.05 (quadratic), and Pr < 0.05 (linear, quadratic) for both colour and S-COD removal. However, the statistical analysis showed that the interaction among parameters was

Table 3
Regression coefficients of the response function for colour and S-COD removal

Coefficient	Values	
	Colour	S-COD
β_0	10.15711	−25.62704
Linear		
β_1	0.50182	1.75973
β_2	0.18769	0.16840
β_3	−0.09752	−0.04907
Quadratic		
β_{11}	0.02634	−0.00457
β_{22}	−0.00017	−0.00015
β_{33}	0.00017	0.00014
Crossproduct		
β_{12}	0.00053	−0.00193
β_{13}	−0.00246	−0.00222
β_{23}	−0.00010	−0.00005

Table 4
ANOVA for the response surface quadratic model for colour and S-COD removal efficiencies

Basis	d.f.[a]	Sum of squares	Mean square	*F*-value	Pr > *F*
Colour removal					
Lack of fit	5	399.34	79.87	5.30	0.05
Pure error	5	75.33	15.07		
Total error	10	474.68	47.47		
S-COD removal					
Lack of fit	5	142.61	28.52	7.13	0.03
Pure error	5	20.00	4.00		
Total error	10	162.61	16.26		

[a] Degrees of freedom.

Table 5
ANOVA of the regression parameters of the predicted response surface quadratic models

Regression	d.f.	Type I sum of squares	R^2	*F*-value	Pr > *F*
Colour removal					
Linear	3	3557.59	0.76	24.98	<0.0001
Quadratic	3	577.11	0.12	4.05	0.0400
Crossproduct	3	92.38	0.02	0.65	0.6015
Total model	9	4227.07	0.90	9.89	0.0007
S-COD removal					
Linear	3	460.20	0.43	9.42	0.0029
Quadratic	3	379.82	0.35	7.79	0.0057
Crossproduct	3	70.38	0.07	1.44	0.2882
Total model	9	910.39	0.85	6.22	0.0043

insignificant in every case. As a result, only linear and quadratic effects of the independent factors were the major determining conditions that might cause considerable effects on the response, while the interaction between the factors were insignificant. This means that all factors considered in this study gave a specific effect on the degradation. However, there were no multiple effects present. The individual effect is more significant than the interaction effect.

Table 6 demonstrates the ANOVA of the independent factors. As can be seen, the recirculation ratio (X_3) was the most significant factor affecting the efficiency of both colour and S-COD removal ($Pr < 0.001$ and 0.005 for colour and S-COD removal efficiency, respectively). Initial H_2O_2 dosage (X_2) was significant to the response of colour removal ($Pr < 0.05$), but only slightly significant to S-COD removal. On the other hand, the irradiation time (X_1) had a less significant effect on both colour and S-COD removal efficiency.

3.2. Analysis of response surfaces

Based on the information from the coded data of the RSREG procedure, a canonical analysis for colour and S-COD removal efficiency indicated that the predicted response surfaces were shaped like a saddle. Therefore, the estimated surfaces did not have a unique optimum. However, the ridge analysis of the response surface indicated that maximum yield will result from a higher initial H_2O_2 dosage as well as a longer irradiation time and a low recirculation ratio.

Eqs. (2) and (3) illustrate the final model equations for dye and S-COD removal efficiencies, respectively. The equations were used to plot the response surfaces

$$Y(\text{dye}, \%) = 10.1571 + 0.5018X_1 + 0.1877X_2 - 0.0975X_3 + 0.0263X_1^2 + 0.0005X_1X_2 - 0.0002X_2^2 - 0.0025X_1X_3 - 0.0001X_2X_3 + 0.0002X_3^2 \quad (2)$$

$$Y(\text{S-COD}, \%) = -25.6270 + 1.7597X_1 + 0.1684X_2 - 0.04907X_3 - 0.0046X_1^2 - 0.0019X_1X_2 - 0.0002X_2^2 - 0.0022X_1X_3 - 0.00005X_2X_3 + 0.0002X_3^2 \quad (3)$$

The response surface and contour plots were made as a function of initial H_2O_2 dosage and recirculation ratio of the system, while keeping the irradiation constant at 20 min (UV irradiation had a less significant effect on the model). The effect of the two variables, namely initial H_2O_2 dosage and recirculation ratio on colour removal efficiency is illustrated in Fig. 3. The recirculation ratio demonstrated a quadratic effect on the response surface at lower H_2O_2 dosage and a linear effect at higher concentration. When irradiation was kept constant at 20 min, the colour removal

Table 6
ANOVA of the factors and the critical values obtained from RIDGE analysis of the response surface for the colour and dye removal

Basis	Analysis of variance					Critical values	
	d.f.	Sum of squares	Mean square	*F*-value	Pr > *F*	Coded	Uncoded
Colour removal							
Irradiation X_1 (min)	4	533.13	133.28	2.81	0.0845	−1.25	7.46
H_2O_2 X_2 (mg/L)	4	955.36	238.84	5.03	0.0175	0.65	427.48
Recirculation X_3 (%)	4	2793.29	698.32	14.71	0.0003	0.52	455.38
S-COD removal							
Irradiation X_1 (min)	4	114.41	28.60	1.76	0.2136	−0.28	17.22
H_2O_2 X_2 (mg/L)	4	207.06	51.77	3.18	0.0626	0.43	385.57
Recirculation X_3 (%)	4	627.25	156.81	9.64	0.0018	0.29	386.61

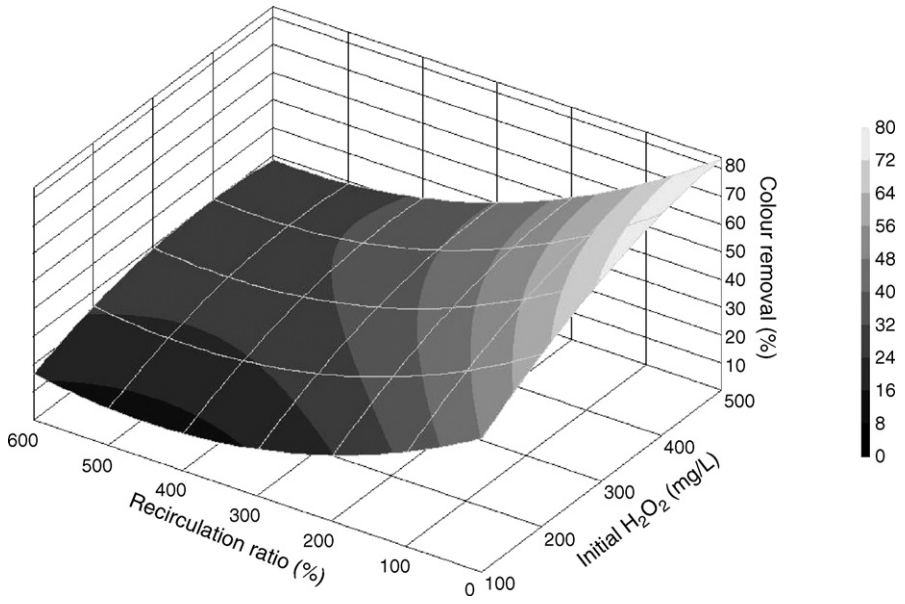

Fig. 3. Response surface plot for the effect of initial H_2O_2 dosage and recirculation ratio on colour removal efficiency at 20 min of UV irradiation.

efficiency decreased with increasing recirculation ratio at almost all initial H_2O_2 dosages examined. The recirculation system was implemented with the aim to improve the efficiency of the system by recycling non-degraded organic molecules from the end of the biological stage to the photoreactor for further chemical oxidation. However, the results of the experimental studies showed that the higher recirculation ratio had a major negative effect on the treatment performance since it diluted the initial H_2O_2 concentration fed into the photoreactor. This dilution seems to have a large effect on the formation of the reactive hydroxyl radicals leading to the dramatic reduction in colour removal observed in the experiments.

At higher recirculation ratios, the efficiency of colour removal slightly increased with increasing dosage of initial H_2O_2 from 100 to 300 mg/L and flattened out at higher initial concentration. When no recirculation was applied, the colour removal increased gradually with increasing H_2O_2 dosage up to 400 mg/L and leveled out afterwards. The decolourisation rate was slow at low H_2O_2 concentrations, as the formation of hydroxyl radicals ($OH^\bullet$) seem to be insufficient. At higher H_2O_2 concentration, more $OH^\bullet$ was produced leading to a faster oxidation rate. At excessively high H_2O_2 concentrations, however, these free radicals may start to react with the excess H_2O_2 rather than with the dye [23,24]. Hydroperoxyl radicals ($HO_2^\bullet$) as the competitive reaction product are much less reactive than $OH^\bullet$ and do not seem to contribute to the decolourisation of RR195A [25,26]

$$H_2O_2 \xrightarrow{h\nu} 2HO^\bullet \quad (4)$$

$$H_2O_2 + HO^\bullet \rightarrow H_2O + HO_2^\bullet \quad (5)$$

$$HO_2^\bullet + HO^\bullet \rightarrow H_2O + O_2 \quad (6)$$

Fig. 4 shows the response surface of the initial H_2O_2 dosage and recirculation ratio on S-COD removal efficiency while irradiation was set at 20 min. The recirculation ratio displayed a quadratic effect on the response at lower initial H_2O_2 dosage concentrations yielding minimum S-COD removal efficiency at 300–400% of the recirculation ratio. Highest S-COD removal efficiencies were always obtained at a recirculation ratio of 0%. There was a linear increase in the COD removal rate with an increasing initial dosage of H_2O_2. However, the higher the initial concentration the more residual H_2O_2 was left in the effluent.

Previous work has suggested that peroxide addition to an activated sludge system will possibly damage the performance of the reactor and lead to the failure of the secondary treatment process. However, it has also been reported that by adding 200 mg H_2O_2/L to an activated sludge system the growth of filamentous bacteria and hence sludge bulking can be avoided [25]. Furthermore, previous investigation have shown that a continuous activated sludge laboratory-scale process is certainly capable of acclimatizing to the presence of hydrogen peroxide (at least up to influent concentrations of 1000 mg/L), while maintaining adequate effluent treatment [26]. Similar results were observed in the present study where there were no signs of a negative impact of the residual H_2O_2 on the bioreactor performance, even at the high initial H_2O_2 concentrations.

Low concentrations of initial H_2O_2 dosage achieved little removal of S-COD, resulting in a considerable amount of non-biodegradable organics entering the bioreactor. This condition occurred especially when higher recirculation ratios were applied to the system. When no recirculation was applied to the system, the S-COD removal efficiency was optimal at an initial H_2O_2 concentration of about 300 mg/L. This initial H_2O_2 concentration seems to provide a good chemical degradation performance without negatively affecting the biological stage.

To perform a colour removal optimization based on Eq. (2) and confirm the results experimentally, a further degradation test was carried out under projected optimal conditions based on the results from the model. Table 7 summarises the decolourisation efficiency for RR195A (100 mg dye/L) using the

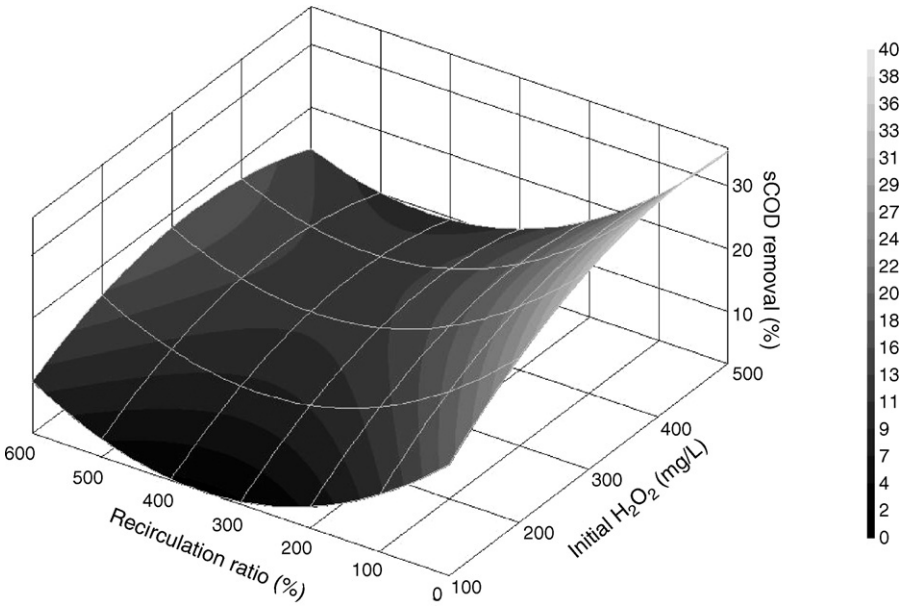

Fig. 4. Response surface plot for the effect of the initial H_2O_2 dosage and recirculation ratio on S-COD removal efficiency at 20 min of UV irradiation.

Table 7
Decolourisation efficiency of RR195A (100 mg dye/L) using the integrated chemical–biological degradation (UV irradiation = 30 min, initial dosage = 100–500 mg H_2O_2/L, no recirculation)

Initial H_2O_2 dosage (mg/L)	Colour removal (%)	Predicted value (%)
100	63	67
200	82	81
300	94	92
400	99	98
500	99	100

integrated chemical–biological process with 30 min of UV irradiation, 100–500 mg H_2O_2/L and no recirculation. The results show clearly that the model predictions for the colour removal efficiency were very close to the actual experimental results and that an initial H_2O_2 dosage of between 300 and 500 mg/L does give a very high degree of dye removal. Considering the additional costs for the higher peroxide concentrations, an initial dosage of 300 mg H_2O_2/L could be regarded as an optimal selection to achieve good dye removal while minimising peroxide addition.

4. Conclusion

The Box–Wilson central composite design and response surface methodology were effective in determining the optimum conditions for decolourisation of RR195A and S-COD removal by the integrated treatment process using UV/H_2O_2 and aerobic biological degradation. Experimental results demonstrated that the dye and S-COD removal efficiency increased from 20 to 86% and 3 to 39%, respectively, by modifying the most influential parameters, in this case UV irradiation time, initial H_2O_2 dosage, and recirculation ratio of the system. The most influential factor identified was the recirculation ratio, whereby a decrease from 600 to 0% led to a distinct improvement in the degradation process. Both longer UV irradiation times and higher peroxide concentrations had a positive effect on dye and S-COD removal efficiencies. Optimal colour degradation conditions predicted from the RSM-based model were well validated by additional experimental results, achieving up to 99% dye removal. This demonstrates the usefulness and effectiveness of the RSM in predicting the system performance and identifies conditions that maximize the dye degradation using the integrated chemical and biological treatment process.

Acknowledgments

The authors would like to thank the Advanced Wastewater Management Centre, The University of Queensland and AusAID Scholarship for supporting the work and the Logan Textile Company, Qld, Australia for providing the dye used in this study.

References

[1] J. Riu, I. Schonsee, D. Barcelo, Determination of sulfonated azo dyes in groundwater and industrial effluents by automated solid-phase extraction followed by capillary electrophoresis/mass spectrometry, J. Mass Spectrom. 33 (1998) 653–663.
[2] I. Peternel, N. Koprivanac, H. Kusic, UV-based processes for reactive azo dye mineralization, Water Res. 40 (2006) 525–532.
[3] V. Lopez-Grimau, M.C. Gutierrez, Decolourisation of simulated reactive dyebath effluents by electrochemical oxidation assisted by UV light, Chemosphere 62 (2006) 106–112.
[4] S. Ledakowicz, M. Solecka, R. Zylla, Biodegradation, decolourisation and detoxification of textile wastewater enhanced by advanced oxidation processes, J. Biotechnol. 89 (2001) 175–184.
[5] R. Krull, M. Hemmi, P. Otto, D.C. Hempel, Combined of biological and chemical treatment of highly concentrated residual dyehouse liquors, Water Sci. Technol. 38 (1998) 339–346.
[6] M. Neamtu, A. Yediler, I. Siminiceanu, M. Macoveanu, A. Kettrup, Decolourization of disperse red 354 azo dye in water by several oxidation process—a comparative study, Dyes Pigments 60 (2004) 61–68.

[7] H. Chun, W. Yizhong, Decolourization and biodegradability of photocatalytic treated azo dyes and wool textile wastewater, Chemosphere 39 (1999) 2107–2115.
[8] F.M. Zhang, J.S. Knapp, K.N. Tapley, Development of bioreactor systems for decolourization of Orange II using white rot fungus, Enzyme Microb. Technol. 24 (1999) 48–53.
[9] T. Robinson, G. McMullan, R. Marchant, P. Nigam, Remediation of dyes in textile effluent: a critical review on current treatment technologies with a proposed alternative, Bioresource Technol. 77 (2001) 247–255.
[10] G.M. Colonna, T. Caronna, B. Marcandalli, Oxidative degradation of dyes by ultraviolet radiation in the presence of hydrogen peroxide, Dyes Pigments 41 (1999) 211–220.
[11] A.M. El-Dein, J.A. Libra, U. Wiesmann, Kinetics of decolourization and mineralization of the azo dye Reactive Black 5 by hydrogen peroxide and UV light, Water Sci. Technol. 44 (2001) 295–301.
[12] V. Lazarova, J. Manem, Advances in biofilm aerobic reactors ensuring effective biofilm activity control, Water Sci. Technol. 29 (1994) 319–327.
[13] W.B. Lui, J.C. Peng, Effects of composition levels on the cellular structure and the thermal properties of biodegradable cushioning extrudates, J Cell. Plast. 40 (2004) 445–459.
[14] M. Linder, N. Kochanowski, J. Fanni, M. Parmentier, Response surface optimisation of lipase-catalysed esterification of glycerol and *n*-3 polyunsaturated fatty acids from salmon oil, Process Biochem. 40 (2005) 273–279.
[15] K. Ravikumar, K. Pakshirajan, T. Swaminathan, K. Balu, Optimization of batch process parameters using response surface methodology for dye removal by a novel adsorbent, Chem. Eng. J. 105 (2005) 131–138.
[16] G.E.P. Box, K.B. Wilson, On the experimental attainment of optimum conditions, J. R. Stat. Soc. Ser. B-Stat. Meth. 13 (1) (1951) 1–45.
[17] W.P. Gardiner, G. Gettinby, Experimental Design Techniques in Statistical Practice: A Practical Software-based Approach, Horwood, England, 1998.
[18] G. Sudarjanto, B. Keller-Lehmann, J. Keller, Photooxidation of a reactive azo-dye from the textile industry using UV/H_2O_2 technology: process optimization and kinetics, J. Water Environ. Technol. 3 (1) (2005) 1–7.
[19] G. Sudarjanto, B. Keller-Lehmann, J. Keller, Colour removal from industrial wastewater using a combination of UV/H_2O_2 and biological process, in: Proceedings of the AWA Ozwater Conference, Brisbane, Australia, 2005.
[20] I.O. Koh, X. Chen-Hamacher, K. Hicke, W. Thiemann, Leachate treatment by the combination of photochemical oxidation with biological process, J. Photochem. Photobiol. A: Chem. 162 (2004) 261–271.
[21] APHA/AWWA/WEF, Standard Methods for the Examination of Water and Wastewater, 19th ed., APHA, Washington, DC, USA, 1995.
[22] R.H. Myers, D.C. Montgomery, Response Surface Methodology: Process and Product Optimization Using Designed Experiments, 2nd ed., Wiley, New York, 2002.
[23] O. Legrini, E. Oliveros, A.M. Braun, Photochemical processes for water treatment, Chem. Rev. 93 (1993) 671–698.
[24] U. Bali, Application of Box–Wilson experimental design method for the photodegradation of textile dyestuff with UV/H_2O_2 process, Dyes Pigments 60 (2004) 187–195.
[25] C.A. Cole, J.B. Stamberg, D.F. Bishop, Hydrogen peroxide cures filamentous growth in activated sludge, J. WPCF 45 (1973) 829–836.
[26] B.C. Larisch, S.J.B. Duff, Effect of H_2O_2 on characteristics and biological treatment of TCF bleached pulp mill effluent, Water Res. 31 (1997) 1694–1706.